© 2018. Published by The Company of Biologists Ltd | Development (2018) 145, dev153858. doi:10.1242/dev.153858

RESEARCH ARTICLE

Differential spatial distribution of miR165/6 determines variability in plant root anatomy

Giovanna Di Ruocco[1,*], Gaia Bertolotti[1,*], Elena Pacifici[1], Laura Polverari[1], Miltos Tsiantis[2], Sabrina Sabatini[1], Paolo Costantino[1,3] and Raffaele Dello Ioio[1,‡]

ABSTRACT

A clear example of interspecific variation is the number of root cortical layers in plants. The genetic mechanisms underlying this variability are poorly understood, partly because of the lack of a convenient model. Here, we demonstrate that *Cardamine hirsuta*, unlike *Arabidopsis thaliana*, has two cortical layers that are patterned during late embryogenesis. We show that a miR165/6-dependent distribution of the HOMEODOMAIN LEUCINE ZIPPER III (HD-ZIPIII) transcription factor PHABULOSA (PHB) controls this pattern. Our findings reveal that interspecies variation in miRNA distribution can determine differences in anatomy in plants.

KEY WORDS: *Cardamine hirsuta*, Ground tissue, HD-ZIPIII, Root development, *Arabidopsis*, miR165/6

INTRODUCTION

A key question in evolutionary genetics is how morphological diversities between species originate. Owing to the high adaptive potential conferred to plants, roots have evolved a variety of anatomical patterns. In fact, roots have largely contributed to the evolutionary success of land plants, enabling them to adapt to different soils and conditions (Fahn, 1990). The cortex is one of the tissues that contributes most to root adaptive potential. In plants living on wet soils, such as rice, secondary growth of the cortex gives rise to the aerenchyma (Fahn, 1990), a tissue controlling the air/water ratio, whereas in plants living in unfavourable conditions, such as turnip, the cortex gives rise to storage parenchyma, a tissue where carbohydrates such as starch are stored (Fahn, 1990). Cortical layer number varies in different plant species ranging from one, as in *Arabidopsis*, to several, as in rice in which it can vary from zero to ten, to horseradish and barley, which have four cortical layers (Heimsch and Seago, 2008; Pauluzzi et al., 2012; Kirschner et al., 2017). Hence, the cortex provides an ideal model system in which to study the genetic mechanisms giving rise to morphological differences in plants.

The cortex, together with the endodermis, forms the root ground tissue (GT). In the *Arabidopsis* root meristem, cortex and endodermis originate from a stem cell (the cortex endodermis initial, CEI); a first asymmetric anticlinal division of the CEI gives rise to a self-renewed stem cell (CEI) and to a daughter cell (CEID). Subsequently, a periclinal division occurs in the CEID and generates endodermis and cortex (Fig. 1A) (Dolan et al., 1993; Benfey et al., 1993; Scheres et al., 1994; Di Laurenzio et al., 1996; Pauluzzi et al., 2012). This mechanism is established during embryogenesis and continues throughout the lifespan of the plant (Dolan et al., 1993; Benfey et al., 1993; Scheres et al., 1994; Pauluzzi et al., 2012).

In *Arabidopsis*, GT patterning is controlled by several genetic pathways that include the genes *SHORTROOT* (*SHR*) and *SCARECROW* (*SCR*), which encode transcription factors, and *CYCLIN D6;1* (*CYCD6;1*) encoding a cell cycle regulator (Helariutta et al., 2000; Pauluzzi et al., 2012; Sozzani et al., 2010; Cruz-Ramírez et al., 2012). The SHR protein is produced in the root vasculature and moves into the endodermis to the CEI and CEID where it is bound and sequestered to the nucleus by SCR and the BIRD zinc finger protein (Cui et al., 2007; Welch et al., 2007; Pauluzzi et al., 2012; Cruz-Ramírez et al., 2012; Long et al., 2015b; Moreno-Risueno et al., 2015; Clark et al., 2016; Long et al., 2017). The SHR/SCR complex in concert with BIRD proteins activates expression of *CYCD6;1* in the CEI, triggering the periclinal division that gives rise to the cortex and the endodermis layers (Sozzani et al., 2010; Pauluzzi et al., 2012; Cruz-Ramírez et al., 2012; Long et al., 2015a,b). It was recently suggested that BIRD proteins act as GT post-embryonic organizers, determining CEI, cortical and endodermal identity (Moreno-Risueno et al., 2015).

MicroRNAs (miRNAs), small non-coding RNAs acting as morphogens in plants (Skopelitis et al., 2012; Baulcombe, 2004), are also involved in GT patterning (Miyashima et al., 2009). miRNA-machinery mutants such as *ago1-102* and *hyl1-2* pattern an extra GT layer during embryogenesis (Miyashima et al., 2009). In *Arabidopsis*, miR165/6 are involved in the spatial restriction of the HOMEODOMAIN LEUCINE ZIPPER III (HD-ZIPIII) transcription factors PHABULOSA (PHB), PHAVOLUTA (PHV), REVOLUTA (REV), CORONA (CNA) and HOMEOBOX GENE 8 (ATHB8) (Mallory et al., 2004). Failure in this restriction generates several developmental anomalies, such as lack of embryo apical/basal and leaf adaxial/abaxial polarity formation, and defects in root zonation and vasculature differentiation (McConnell et al., 2001; Grigg et al., 2009; Dello Ioio et al., 2012; Carlsbecker et al., 2010). In the *Arabidopsis* root, the SHR transcription factor regulates *MIR165/6* expression, restricting in a dose-dependent fashion HD-ZIPIII gene expression to the stele: this generates a radial gradient of HD-ZIPIII gene expression in the root vasculature, which patterns the stele (Carlsbecker et al., 2010). It was also posited that maintenance of the HD-ZIPIII expression gradient is necessary to restrict the *Arabidopsis* GT to one cortex and one endodermis, as a miR165/6-resistant version of PHB promotes the formation of extra GT layers (Miyashima et al., 2011). Although these mechanisms limiting GT development to one cortex and one

[1]Department of Biology and Biotechnology, Laboratory of Functional Genomics and Proteomics of Model Systems, Sapienza University of Rome, via dei Sardi, 70-00185 Rome, Italy. [2]Department of Comparative Development and Genetics, Max Planck Institute for Plant Breeding Research, Carl-von-Linné-Weg 10, 50829 Köln, Germany. [3]Dipartimento Biologia e Biotecnologie and Consiglio Nazionale delle Ricerche, Istituto Biologia e Patologia Molecolari, Sapienza Università di Roma, 00185 Roma, Italy.
*These authors contributed equally to this work

‡Author for correspondence (raffaele.delloioio@uniroma1.it)

R.D., 0000-0001-8679-9412

Received 26 April 2017; Accepted 9 November 2017

Development (2018) 145, dev153858. doi:10.1242/dev.153858

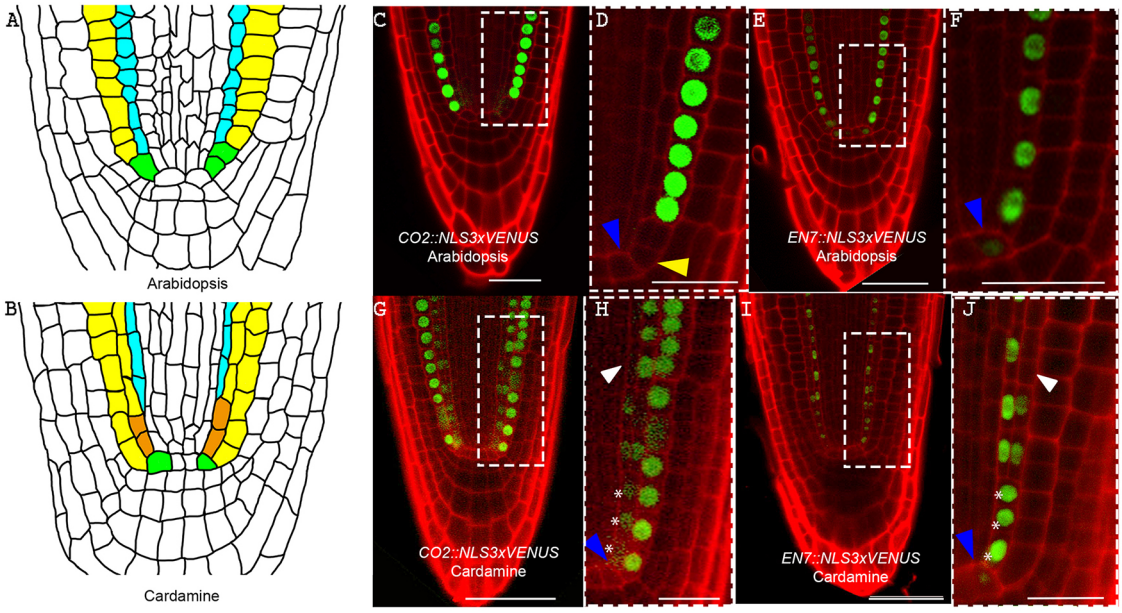

Fig. 1. *Cardamine* has two cortical and one endodermis layers patterned during embryogenesis. (A) Diagram of *Arabidopsis* root meristem. The CEI/CEID is shown in green, the endodermis in cyan, the cortex in yellow. (B) Diagram of *Cardamine* root meristem. The CEI is shown in green, the CEM in orange, the endodermis in cyan, the cortex in yellow. (C) Confocal image of an *Arabidopsis CO2::NLS3xVENUS* meristem at 4 days post-germination (dpg) (*n*=11). (D) Magnification of the boxed region in C. (E) Confocal image of an *Arabidopsis EN7::NLS3xVENUS* meristem at 4 dpg (*n*=8). (F) Magnification of the boxed region in E. (G) Confocal image of a *Cardamine CO2::NLS3xVENUS* meristem at 4 dpg (*n*=25). (H) Magnification of the boxed region in G. (I) Confocal image of a *Cardamine EN7::NLS3xVENUS* meristem at 4 dpg (*n*=15). (J) Magnification of the boxed region in I. Propidium iodide is in red, VENUS in green. White asterisks indicate the CEM, white arrowheads indicate the first cells without fluorescence, blue arrowheads indicate the CEI, yellow arrowhead indicates the CEID. Scale bars: 50 µm (C,E,G,I); 20 µm (D,F,H,J).

endodermis layer are fairly well-characterized in *Arabidopsis*, how differences in cortical layer number among species are generated is still uncertain. One possibility is that SHR might control layer number in multiple-cortex species, such as *Oryza sativa* or *Brachypodium distachyon*, as the expression of the *SHR* locus of these species generates multiple cortical layers in *Arabidopsis* (Wu et al., 2014). However, whether this and/or other pathways control the variability of cortical layer number between species is still not established, partly owing to the lack of a convenient multiple-cortex root model system related to *Arabidopsis*.

To address this question, we utilized *Cardamine hirsuta*, a genetically tractable close relative of *Arabidopsis* and a well-established model plant for comparative development studies of shoot organs (Hay and Tsiantis, 2006; Vlad et al., 2014; Rast-Somssich et al., 2015; Hofhuis et al., 2016; Vuolo et al., 2016). We demonstrate that *Cardamine* has two root cortical layers (outer and inner) and one endodermis layer that are pre-patterned during embryogenesis. We show that the inner root cortical layer in *Cardamine* originates from a tissue with mixed cortical/endodermal identity that we called CEM. Through a comparative analysis of root development, we provide evidence that a differential spatial distribution of the transcription factor PHB and of miR165/6 are responsible for the cortex anatomical differences between *Arabidopsis* and *Cardamine* regulating CEM activity.

RESULTS

Cardamine has two cortical layers patterned during embryogenesis

It was previously shown that *Cardamine* has an additional GT layer compared with *Arabidopsis* (Fig. 1A,B) (Hay et al., 2014).

To determine the identity of this additional GT layer, we utilized fluorescent constructs of two GT markers: *CORTEX2* (*CO2*), which is specific for the cortical layer, and *ENDODERMIS7* (*EN7*), which is expressed only in the endodermis (Heidstra et al., 2004). As expected, in *Arabidopsis CO2::NLS3xVENUS* had a maximum expression in the cortex and is excluded from the CEI, CEID and the quiescent centre (QC) (Fig. 1C,D). In *Arabidopsis EN7::NLS3xVENUS* plants, fluorescence is detectable in the inner GT layer including the CEI and is excluded from the QC (Fig. 1E,F). In *Cardamine*, *CO2::NLS3xVENUS* expression is detectable in both the outer and the middle layer of the GT and is excluded from CEI and QC, whereas in *EN7::NLS3xVENUS* plants we could detect fluorescence only in the inner layer of the GT and in the CEI but not in the QC, pointing to the presence of a single endodermis and two cortical layers (Fig. 1G-J). Consistent with these data, *Cardamine* roots present only one casparian strip as visualized by endodermis-specific suberin autofluorescence (Fig. S1A-F).

We also noticed that in the *Cardamine* post-embryonic root at a two- to three-cell distance from the QC, a GT cell divides periclinally generating the inner cortical layer (Fig. S1G,H). We analysed the identity of those cells and we observed that the GT cells preceding the division that originates the second cortical layer in *Cardamine* express reporters of both cortex and endodermis, suggesting that they have a mixed identity; thus, we called this domain CEM (cortex/endodermis mix) (Fig. 1B,H,J). The cells deriving from the second GT periclinal division show the fluorescence of both *EN7::NLS3xVENUS* and *CO2::NLS3xVENUS* constructs, probably because of the stability of the NLS-3xVENUS protein (Wysocka-Diller et al., 2000). At a two-cell distance from the periclinal division of the endodermis, the middle GT cells lose endodermis identity and maintain cortical identity (Fig. 1H,J).

To establish whether the *Cardamine* double cortical layer is patterned during embryogenesis or after its completion, we analysed GT embryonic development. Based on *Arabidopsis*, we considered

Development (2018) 145, dev153858. doi:10.1242/dev.153858

as root meristem GT the portion of GT contained within the lateral root cap (Dolan et al., 1993; Scheres et al., 1994).

We observed that, like in *Arabidopsis*, in the first stages of *Cardamine* embryogenesis the root GT develops as a monolayer that forms one cortex and one endodermis at heart stage, and two cortical layers in the hypocotyl (Fig. 2A,B,G,H). However, unlike *Arabidopsis*, an additional periclinal division in the endodermis at late torpedo stage gives rise to a second cortical layer that is then maintained throughout the life of the plant (Fig. 2C-F,I,J). We also noticed that an additional periclinal division occurs in the hypocotyl of *Cardamine* embryos from the late torpedo stage onwards, which increases the number of cortical layers to three (Fig. 2C-F). Using high-resolution modified pseudo-Schiff-propidium iodide (mPS-PI) staining (Truernit et al., 2008), we observed that CEI division produces the outer cortical layer and inner CEM cells. The latter divides giving rise to the inner cortex and the endodermis, in a similar fashion to post-embryonic development (Fig. 2K,L).

PHB and PHV HD-ZIPIII transcription factors regulate cortex patterning in *Arabidopsis*

To unravel the genetic mechanisms driving the formation of the two cortical layers in *Cardamine*, we performed a comparative analysis with *Arabidopsis*. We noticed that among *Arabidopsis* mutants showing additional root layers, *ago1* and *hyl1* develop an extra GT layer during embryogenesis (Paquette and Benfey, 2005; Heo et al., 2011; Zhang et al., 2011; Miyashima et al., 2009), resembling *Cardamine* GT patterning. We examined the *hyl1-1* mutant and an additional hypomorphic allele of *ago1* (*ago1-27*) in *Arabidopsis*, which show an extra GT layer patterned during embryogenesis (Fig. 3A-D; Fig. S2A,C,E,G). Moreover, we found that mutation in *HASTY*, another member of the miRNA biogenesis machinery (Park et al., 2005), also generates an additional GT layer during embryogenesis (Fig. S2I,K). We characterized the identity of this additional layer in *hyl1* mutants, as an example of this set of mutants, utilizing *CO2::H2B:YFP* and *EN7::H2B:YFP* (Heidstra et al., 2004), where CO2 and EN7 promoters drive the expression of the HISTONE2B (H2B) fused to yellow fluorescent protein (YFP). We could detect the fluorescent signal of the *CO2::H2B:YFP* in the outer GT layers and of the *EN7::H2B:YFP* in the inner GT layer of *hyl1-1* mutants (Fig. S3), suggesting that variations in miRNA biogenesis results in formation of supernumerary cortical layers.

The miR165/6-insensitive mutants of the redundantly acting *PHB* and *PHV* genes, *phb-1d* and *phv-1d*, express these genes also in the GT and show an extra GT layer (Miyashima et al., 2011). Nevertheless, whether the broader expression of PHB and PHV generates the additional GT layer in miRNA biogenesis loss-of-function mutants is not known. To assess this, we analysed the activity of the XPHB sensor of miR165/6, a constitutively expressed green fluorescent protein (GFP) sensitive to miR165/6 (Dello Ioio et al., 2012) in the *hyl1-1* background. Unlike in wild-type (Wt) plants, we detected GFP expression in the GT of *hyl1-1*, suggesting a peripheral broadening of the PHB and PHV gradient (Fig. S4). Consistent with this evidence, the triple loss-of-function mutants *hyl1-1;phb-13;phv-11*, *hst-1;phb-13;phv-11* and *ago1-27;phb-13;phv-11* display only one cortex and one endodermis layer already from embryogenesis in a similar fashion to Wt and *phb-13;phv-11*

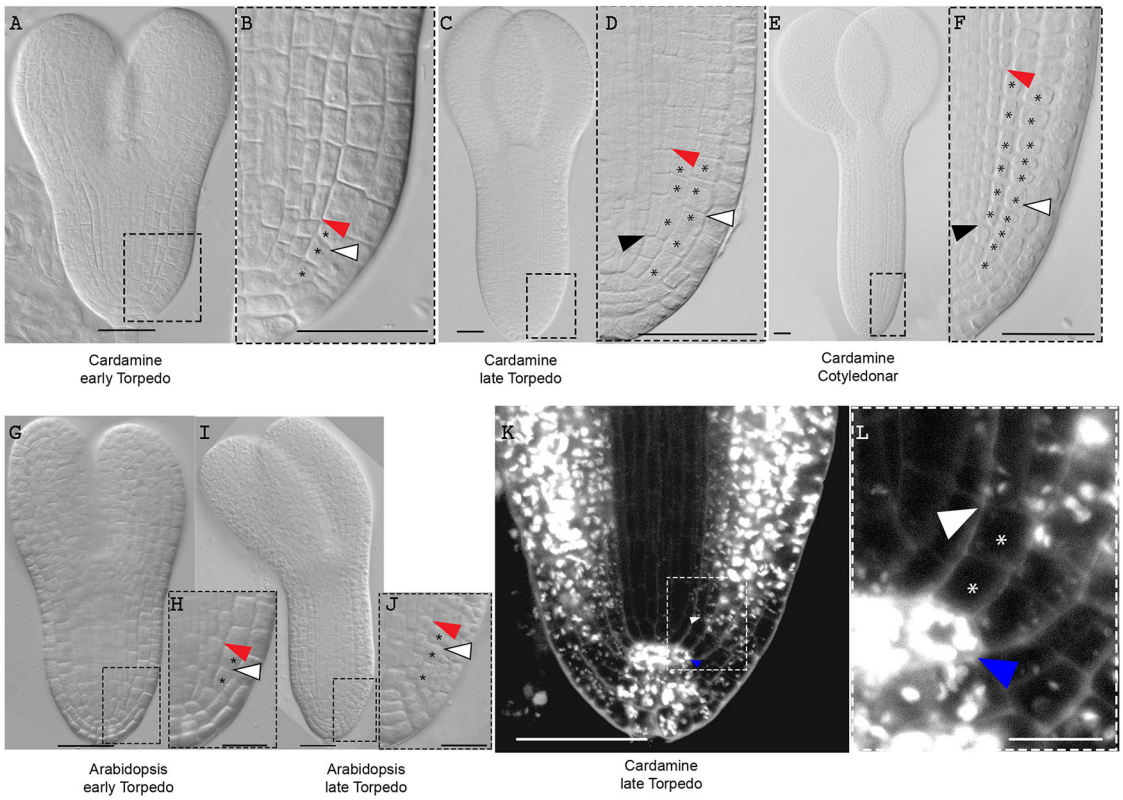

Fig. 2. *Cardamine* inner cortical layer is patterned during embryogenesis. (A-J) DIC images of *Cardamine* and *Arabidopsis* embryos at the reported developmental stages (A,C,E,G,I) and the respective magnifications of the boxed regions (B,D,F,H,J) (respectively, *n*=12, *n*=15, *n*=14, *n*=7, *n*=8). White arrowheads indicate the root meristem border, black asterisks indicate cortical layers, black arrowheads indicate the CEM division, red arrowheads indicate hypocotyl periclinal division. (K,L) mPS-PI images of a *Cardamine* embryo at the reported developmental stage (*n*=18) (K) and the magnification of the boxed region in K (L). Blue arrowheads indicate the CEI. White arrowheads indicate the CEM division. White asterisks indicate CEM. Scale bars: 50 µm (A,C,E,G,I,K); 20 µm (B,D,F,H,J,L).

Development (2018) 145, dev153858. doi:10.1242/dev.153858

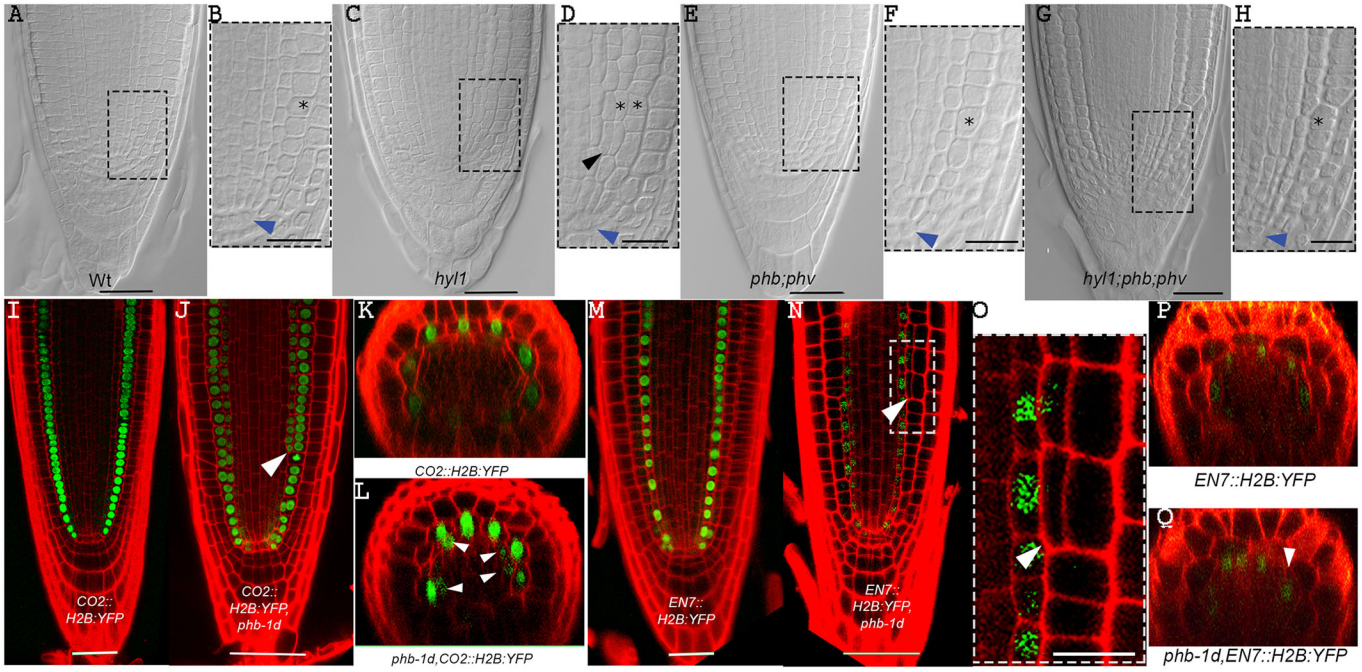

Fig. 3. PHB ectopic activity outputs in additional cortical layers. (A-F) DIC images of root meristems of Wt (*n*=8) (A), *hyl1-1* (*n*=18) (C), *phb-13;phv-11* (*n*=6) (E) and *hyl1-1;phb-13;phv-11* (*n*=14) (G) plants at 5 dpg and the respective magnifications of the boxed areas (B,D,F,H). Blue arrowheads indicate the CEI, black arrowheads the extra periclinal division, asterisks the cortical layer(s). (I,J) Confocal images of root meristems of *CO2::H2B:YFP* Wt (*n*=10) (I) and *phb-1d* (*n*=14) (J) plants at 5 dpg. (K,L) Transverse sections of the root meristem of *CO2::H2B:YFP* Wt (*n*=4) (K) and *phb-1d* (*n*=4) (L). (M,N) Confocal images of root meristems of *EN7::H2B:YFP* Wt (*n*=6) (M) and *phb-1d* (*n*=20) (N) plants at 5 dpg. (O) Magnification of the boxed region in N. (P,Q) Transverse sections of the root meristem of *EN7::H2B:YFP* Wt (*n*=4) (P) and *phb-1d* (*n*=3) (Q). White arrowheads indicate the extra periclinal division. Propidium iodide is in red, YFP in green. Scale bars: 50 µm (A,C,E,G,I,J,M,N); 20 µm (B,D,F,H,O).

mutant plants (Fig. 3A-H; Fig. S2) suggesting that ectopic expression of PHB and PHV is required to generate the extra-cortical layer in *hyl1-1*, *hst-1* and *ago1-27 Arabidopsis* backgrounds.

To characterize the identity of the additional GT layer of *phb-1d* and *phv-1d* mutants, we analysed the reporter activity of *CO2::H2B:YFP* and *EN7::H2B:YFP* in those backgrounds. In both genotypes, the *CO2::H2B:YFP* signal was consistently detected in the additional GT layer whereas the *EN7::H2B:YFP* was randomly expressed in only a subset of these cells, suggesting that this additional GT layer has cortex identity (Fig. 3I-Q; data not shown). We concluded that the expansion of PHB domain in the GT generates an additional cortical layer.

HD-ZIPIII transcription factors control cortex patterning in *Cardamine*

Because of the capability of the PHB and PHV HD-ZIPIII transcription factors to control cortical layer number in *Arabidopsis*, we hypothesized that these factors might be responsible for the generation of the double cortical layer in *Cardamine*. We identified five orthologues of the *Arabidopsis* HD-ZIPIII genes in the genome of *Cardamine* (Gan et al., 2016), which we named *ChPHB*, *ChPHV*, *ChREV*, *ChHB8*, *ChCNA* (Fig. S5A). Sequence alignment showed that the *Ch*HD-ZIPIII genes are all more than 90% similar to *Arabidopsis* and that all of them contain a miR165/6 recognition site domain (Fig. S5). We also found that the *Arabidopsis* nine *miR165/6* loci are conserved in the *Cardamine* genome and their alignment showed that the processed miR165 and miR166 sequences are 100% homologous to the *Arabidopsis* counterpart (Fig. S5B). To assess whether the HD-ZIPIII proteins control double cortex formation in *Cardamine*, we knocked down the HD-ZIPIII genes by means of the expression of the precursor of miR165, *pri-MIR165A*, driven by the *35S* promoter (*35S::MIR165A*). Out of 16 independent *35S::MIR165A Cardamine* lines, 14 showed one cortex and lack of CEM in the T1 generation suggesting that HD-ZIPIII transcription factors are necessary for double cortex formation in *Cardamine* (Fig. 4A-C).

Previous reports have shown, via a GFP translational fusion (*AtPHB:GFP*), that in *Arabidopsis* PHB expression is restricted to the stele (Fig. 4I,K; Fig. S7A) (Carlsbecker et al., 2010; Miyashima et al., 2011; Dello Ioio et al., 2012). To establish whether HD-ZIPIII proteins present a different spatial distribution between *Arabidopsis* and *Cardamine*, we analysed the expression of a translational fusion *ChPHB:GFP* in *Cardamine* root, focusing on *PHB* because its ectopic expression is sufficient to induce the formation of an additional cortical layer in *Arabidopsis* (Fig. 3). We observed that *ChPHB:GFP* fluorescence is present in the vasculature, QC, CEI/CEID and in the CEM of *Cardamine* root (Fig. 4D,E), whereas in *Arabidopsis* root *AtPHB:GFP* is localized only in the vasculature (Fig. S7A) (Carlsbecker et al., 2010; Miyashima et al., 2011; Dello Ioio et al., 2012). These results suggest that the presence of the PHB transcription factor in the GT of *Cardamine* is responsible for the additional cortical layer (Fig. 4I,K).

miRNA165/6 distribution generates diversity in cortical layer number

We have suggested that in *Cardamine* the presence of PHB in the GT is responsible for the double cortical layer. Because in *Arabidopsis* it is the activity of miR165/6 in the GT that restricts PHB expression to the stele (Fig. 4I,K) (Carlsbecker et al., 2010; Miyashima et al., 2011), we investigated the hypothesis that the lack of miR165/6 in the *Cardamine* GT allows the broadening of the PHB domain. Consistent with this hypothesis, we observed that decreasing

Development (2018) 145, dev153858. doi:10.1242/dev.153858

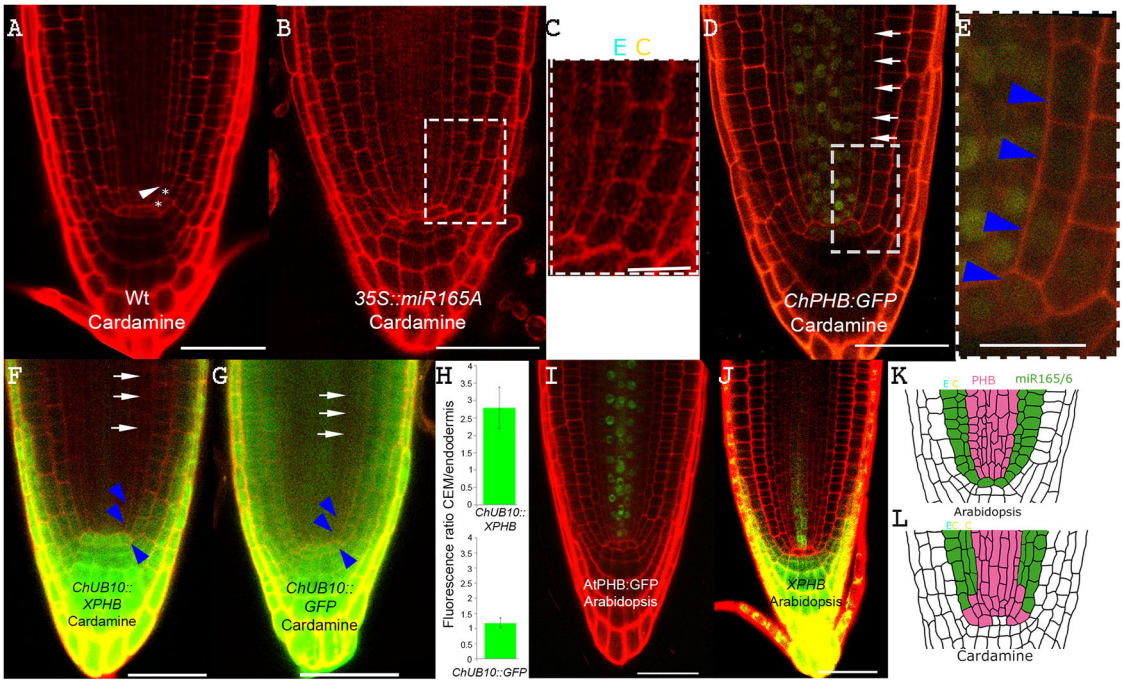

Fig. 4. PHB and miR165/6 have different activity domains between *Cardamine* and *Arabidopsis*. (A,B) Confocal images of root meristem Wt (*n*=5) (A) and *35S::miR165A* (*n*=16) (B) *Cardamine* plants at 5 dpg. White asterisks indicate the CEM, white arrowhead indicates the second periclinal division. (C) Magnification of the boxed region in B. (D) Confocal image of 2 dpg Wt *Cardamine* root harbouring a *ChPHB:GFP* construct (*n*=8). (E) Magnification of the boxed region in D. (F) Confocal image of 3 dpg Wt *Cardamine* root harbouring a *ChUB10::XPHB* construct (*n*=15). (G) Confocal image of a 2 dpg *ChUB10::GFP Cardamine* plant (*n*=10). *ChUB10::GFP* plants are used as control of *ChUB10* expression domain. White arrows indicate the endodermis, blue arrowheads the CEI and the CEM. (H) Graph depicting the green fluorescence ratio between three cells of the CEM and three cells of endodermis in *ChUB10::XPHB* and in *ChUB10::GFP* plants. Each fluorescence value was normalized to the corresponding cell area. *n*=6. Error bars represent s.d. (I) Confocal image of 2 dpg Wt *Arabidopsis* root harbouring a *AtPHB:GFP* construct (*n*=5). (J) Confocal image of 5 dpg Wt *Arabidopsis* root harbouring a *XPHB* construct (*n*=10). (K) Diagram of the pattern domain of PHB (pink) and miR165/6 (green) in *Arabidopsis*. (L) Diagram of the distribution of PHB (pink) and miR165/6 (green) in *Cardamine*. White arrows indicate the endodermis. Scale bars: 50 µm (A,B,D,F,G); 20 µm (C,E). GFP signal is in green, propidium iodide signal is in red. C, cortex; E, endodermis.

miR165/6 activity in the *Arabidopsis* GT, by expressing a DNA fragment mimicking the miR165/6 target sequence (*35S::MIM165/6*) (Todesco et al., 2010), produces a broader XPHB signal and an extra cortical layer (Fig. S6). This suggests that the expression of *PHB* in this background is no longer restricted to the stele and links this phenomenon to the formation of a second cortex. To establish whether miR165/6 activity is indeed absent from *Cardamine* GT, we generated *Cardamine* plants harbouring the XPHB miR165/6-sensitive GFP protein under the control of the *Cardamine* constitutive promoter *ChUbiquitin10* (*ChUB10::XPHB*). We could detect GFP signal in the QC, CEI, CEID and CEM, suggesting that activity of miR165/6 is low in these cells (Fig. 4F-H). By contrast, we detected low GFP fluorescence in the endodermis, indicating that miR165/6 is active in those cells (Fig. 4F-H). Hence, the broader expression domain of *PHB* in *Cardamine* compared with *Arabidopsis* might be dependent on the different miR165/6 activity domain in the two species (Fig. 4K,L). To verify that the presence of the PHB protein in the *Cardamine* GT is actually due to the absence of miR165/6 in the endodermis and not to an intrinsic property of the *Cardamine* PHB protein, we analysed the expression of the *ChPHB:GFP* construct in *Arabidopsis*. In these plants, the distribution of the *ChPHB:GFP* protein mirrors that of *AtPHB:GFP* (Fig. S7A,B), suggesting that the presence of miRNA166 in the *Arabidopsis* GT is sufficient to restrict PHB in the stele. Conversely, expression of the miR165/6-insensitive form of PHB (*AtPHB*:GFP*) in *Arabidopsis* is expanded in the endodermis and is accompanied by the formation of extra GT layers (Fig. S7C-E).

These results suggest that the absence of miR165/6 in the *Cardamine* root GT allows expression of PHB in the GT, which results in the development of an extra cortical layer.

PHB controls GT patterning via CYCD6;1

It was recently reported that *Arabidopsis* plants expressing the rice and *Brachypodium SHR* locus show extra cortical layers (Wu et al., 2014). To understand whether *Cardamine* SHR also generates additional cortical layers in *Arabidopsis*, we created a construct in which *ChSHR* is fused to cyano fluorescent protein (CFP) (*ChSHR:CFP*). We observed that *Arabidopsis* plants harbouring *ChSHR:CFP* display an additional GT layer and that *ChSHR:CFP* is sufficient to both recover the *shr-1* phenotype (55%) or induce additional GT layers in the latter background (45%) (Fig. S8A-C), suggesting a conserved function of SHR in determining cortical layer number in different species.

To assess possible links between the SHR and PHB pathways in GT patterning, we generated *ChSHR:CFP;phb-13;phv-11 Arabidopsis* lines. Loss of *PHB* and *PHV* activity was not sufficient to suppress the *ChSHR:CFP* phenotype completely (Fig. S8A-D), indicating that PHB and PHV are not required for the SHR GT-patterning action.

To determine whether PHB requires SHR to induce extra cortex formation, we generated double mutants *shr-1;phb-1d.* As visualized by the activity of the cortex marker *CO2::H2B:YFP*, these plants show a double cortical layer, similar to *phb-1d* single mutants (Fig. S8H-M), suggesting that the effect of PHB on GT development does not require SHR. These results suggest that the

Development (2018) 145, dev153858. doi:10.1242/dev.153858

SHR and PHB pathways act in parallel in controlling cortical layer number.

The cyclin CYCD6;1 controls the periclinal division of the CEID that gives rise to cortex and endodermis (Sozzani et al., 2010). To assess whether, in analogy with SHR/SCR, PHB acts on the *CYCD6;1* gene in the formation of extra cortical layers, we analysed *CYCD6;1* expression in the *phb-1d* mutant, which expresses *PHB* also in the GT. qRT-PCR analysis showed an increased level of *CYCD6;1* mRNA in *phb-1d* roots (Fig. 5A), suggesting that the expression of *CYCD6;1* is regulated by PHB. To understand whether CYCD6;1 induction by PHB coincides with second cortex formation, we analysed a fluorescent transcriptional reporter of CYCD6;1 (*CYCD6;1::GFP:GUS*) in the *phb-1d* background. Whereas in Wt roots *CYCD6;1::GFP:GUS* has a maximum fluorescent signal in the CEI/CEID, in *phb-1d* we could detect high *CYCD6;1* activity also at the additional division site that generates the second cortex formation in *phb-1d* background (Fig. 5B,C). This indicates that, although independent of one another, the PHB and SHR/SCR pathways both act on *CYCD6;1* expression in patterning the GT.

In *Arabidopsis*, SHR and SCR control CYCD6;1 expression in the GT (Sozzani et al., 2010; Cruz-Ramírez et al., 2012). To assess whether PHB regulates CYCD6;1 expression independently of the SHR/SCR pathway, we measured CYCD6;1 mRNA levels in *phb-1d; shr-1* background by qRT PCR. In the *shr* background *CYCD6;1* expression is almost undetectable (Koizumi et al., 2012). The *phb-1d* mutation is sufficient to increase *CYCD6;1* mRNA levels in the *phb-1d;shr-1* background (Fig. S8O), suggesting that PHB controls CYCD6;1 expression independently of SHR. A 4 h induction of a dexamethasone (DEX)-inducible miRNA-resistant version of PHB (*35S:GR≫PHB**) results in a mild but significant increase of *CYCD6;1* mRNA level in this background (Fig. S8P), suggesting that CYCD6;1 is an early, but most likely not direct, target of PHB.

DISCUSSION

We showed that the *Cardamine* double cortical layer originates from a developmental domain of mixed cortical and endodermal identity, the CEM, established during embryogenesis. Our results suggest that the presence of PHB in the CEM is necessary and sufficient to generate an additional cortical layer in the *Cardamine* GT. In the CEM, PHB might regulate the expression of *CYCD6;1* triggering an additional periclinal division in the GT (Fig. 5D). Whereas in *Arabidopsis*, miR165/6 activity in QC, CEI/CEID, endodermis and cortex clears out *PHB* mRNA from the GT, in *Cardamine* the PHB protein is present in the GT owing to the absence of miR165/6 activity in those cells (Fig. 5D). Thus, the difference in GT patterning between *Arabidopsis* and *Cardamine* seems to result from a difference in the localization of miR165/6, which generates a different distribution of PHB in the two species. Our data also suggest that in *Cardamine* post-embryonic root development the presence of miR165/6 activity in differentiated endodermis eliminates PHB from this tissue, thus suppressing the formation of additional periclinal divisions and maintaining the number of cortical layers.

Our results highlight the role of HD-ZIPIII in the control of cortical layer number. Further studies on multi-cortical layer model species will clarify whether this mechanism holds true in general for plant root cortical variability.

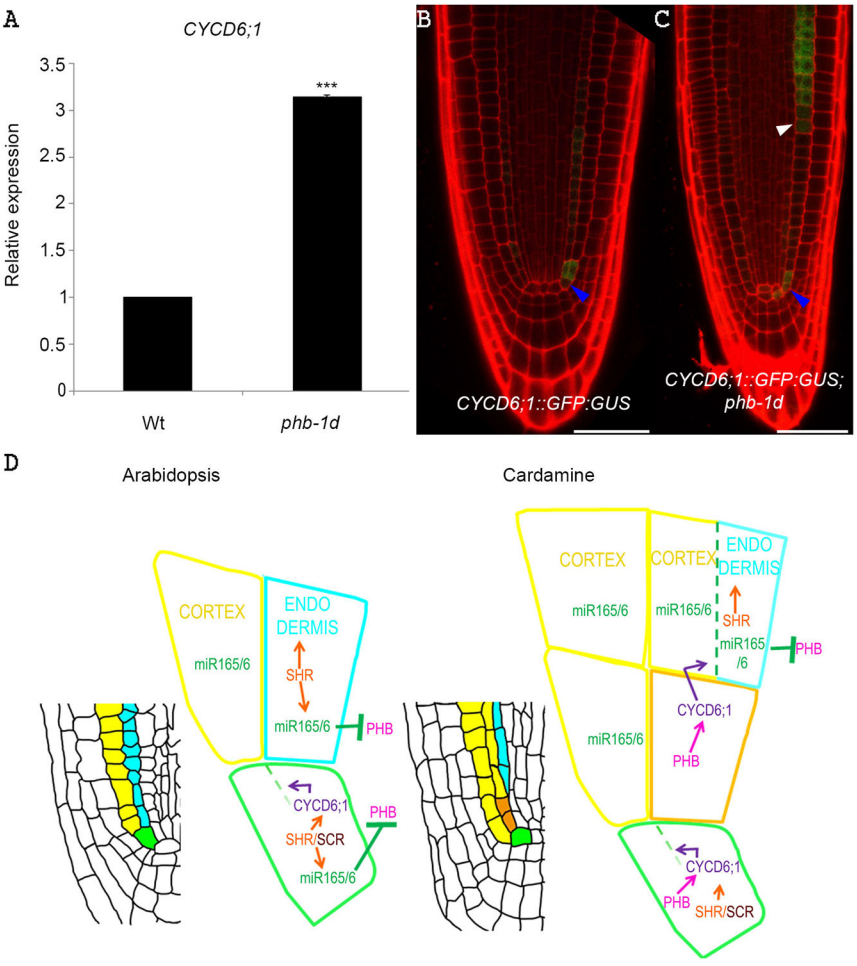

Fig. 5. PHB controls *CYCD6;1* expression in *Arabidopsis*. (A) qRT-PCR of *CYCD6;1* in Wt and *phb-1d* roots. $n=2$, $^{***}P<0.01$. Error bars represent s.d. (B,C) Confocal images of root meristem of Wt ($n=8$) (B) and *phb-1d* mutant ($n=9$) (C) plants at 5 dpg, carrying the *CYCD6;1::GFP:GUS* construct. Propidium iodide is in red, GFP is in green. White arrowhead indicates the additional periclinal division in the GT, blue arrowheads indicate the CEI. (D) Schematic of the proposed model. In *Arabidopsis*, the activity of SHR and SCR in the CEI (green) is necessary and sufficient to induce *CYCD6;1* expression, promoting the periclinal division (dashed green line) that gives rise to cortex (yellow) and endodermis (cyan). In the CEI/CEID and endodermis, SHR induces miR165/6, which restricts PHB expression to the stele. In *Cardamine*, the activity of PHB in the CEI and in the CEM tissue (orange) stimulates *CYCD6;1* expression in these cells, promoting an additional periclinal division (dashed green line). This additional periclinal division produces the extra cortex layer (yellow half). Subsequently, miR165/6 is active in the endodermis (cyan), restricting PHB to the stele.

Development (2018) 145, dev153858. doi:10.1242/dev.153858

In *Arabidopsis* embryos, miR165A expression is independent of SHR (Miyashima et al., 2013). In a similar fashion, we posit that the SHR/SCR regulatory circuit might not activate miR165/6 expression in the *Cardamine* QC, CEI and CEM (Fig. 5D). Consistent with this hypothesis, *Ch*SCR, a conserved SHR target (Cui et al., 2007), is expressed in tissues in which miR165/6 activity is not detectable, such as CEI and CEM, as visualized by a *ChSCR* regulative sequence fused to GFP targeted to the endoplasmic reticulum, ERGFP (Fig. S8N; *ChSCR::ERGFP*). Hence, miR165/6 expression might be SHR dependent only in the endodermis where we detect miR165/6 activity but not in the CEI/CEID, CEM and QC. Analysis of the expression of the four miR165/6 and cross-species experiments between *Arabidopsis* and *Cardamine* will help to clarify the role of SHR in regulating the expression of these miRNAs in *Cardamine* GT. We provided evidence in *Arabidopsis* that PHB regulates additional cortical layers via the control CYCD6;1 expression independently of SHR/SCR. Our results do not rule out the possibility that the PHB and SHR/SCR circuits may interconnect downstream, as a reduction in *CYCD6;1* mRNA level is still detectable in *shr,phb-1d* background compared with *phb-1d* single mutants (Fig. 5A; Fig. S8O). It was recently shown that the SHR protein is detectable in rice root cortical layers, and that overexpression of *Arabidopsis* SHR increases the number of cortical layers in rice (Henry et al., 2017). Our results raise the possibility that PHB controls the expression of *CYCD6;1* via induction of a third as-yet-unidentified component, as short induction of PHB increases *CYCD6;1* expression only slightly. Further studies in *Arabidopsis* and *Cardamine* will be required for a better understanding of the connection between these two pathways in GT patterning.

It remains to be established whether, through the control of CYCD6;1, the MIR165/6/PHB circuit generates the CEM or regulates its activity, and additional work is required to elucidate fully the genetic network leading to double cortex formation in *Cardamine*. However, our results indicate that variations in miRNA distribution are capable of determining differences in plant anatomy.

MATERIALS AND METHODS

Growth conditions

Arabidopsis and *Cardamine* seeds were surface sterilized using a solution containing 70% ethanol and 0.5% Triton X-100 (Carlo Erba) for 10 min and then with a solution of 96% ethanol for 10 min. Seeds were air dried and suspended in 0.1% agarose in water. *Arabidopsis* seeds were plated after 3 days of cold treatment, *Cardamine* seeds after 5 days. Seeds were grown in a vertical position, at 22°C in 16 h light/8 h dark cycle, on ½ MS (Murashige and Skoog medium, Duchefa) supplemented with 1% sucrose, as described by Perilli and Sabatini (2010).

Plant material

All *Arabidopsis* material is in Columbia ecotype, all *Cardamine* lines are in Oxford ecotype. *CO2::H2B:YFP* and *EN7::H2B:YFP* were kindly donated by R. Heidstra (Heidstra et al., 2004). *CYCD6;1::GFP:GUS* line was kindly given by R. Sozzani (Sozzani et al., 2010). *phb-1d/+*, *phv-1d/+* (used in this study), *XPHB*, *XmPHB*, *PHB*:GFP*, *PHB:GFP*, 35S:GR≫PHB* were previously described by Dello Ioio et al. (2012), *phb-13;phv-11* by Prigge et al. (2005), *ago1-27* by Morel et al. (2002), *hyl1-1* by Lu and Fedoroff (2000), *hst1-1* by Telfer and Poethig (1998) and *shr-1* by Scheres et al. (1995). Primers used for genotyping are listed in Table S1. Approximately 20 plants for genotype were analysed.

Transgenic lines generation

CO2::3xNLSVENUS and *EN7::3xNLSVENUS* were constructed by excising the promoters from *CO2::H2B:YFP* and *EN7::H2B:YFP* plasmids utilizing *Xho*I and *Bam*HI sites. The CO2 and EN7 promoter were subsequently inserted in a 3xNLSVENUS-PBJ36 plasmid. *CO2::NLS3xVENUS* and *EN7::NLS3xVENUS* cassettes were inserted in a pMLBART plasmid utilizing *Not*I sites.

ChPHB:GFP and *ChSHR:CFP* constructs were generated utilizing the Gateway system (Invitrogen). The 3 kb region upstream of the *ChPHB* ATG and the *ChPHB* genomic sequence without the stop codon were amplified from *Cardamine* and cloned respectively in pDONR_P4_P1R and pDONR221 Gateway vector by BP recombination (Invitrogen). Subsequently, pDONRP4_P1R-ChPHBp and pDONR221-ChPHB were recombined with pDONR P2R_P3-C-term GFP into a pB7m34GW destination vector via LR reaction (Invitrogen; Karimi et al., 2002). The 2.9 kb *ChSHR* region upstream of the *ChSHR* ATG and the *ChSHR* genomic sequence without stop codon were amplified from *Cardamine* and cloned respectively in a pDONR_P4_P1R and a pDONR221 Gateway vector by BP recombination (Invitrogen). Subsequently, pDONRP4_P1R-ChSHRp and pDONR221-ChSHR were recombined with pDONR P2R_P3-C-term CFP into a pB7m34GW destination vector via LR reaction (Invitrogen; Karimi et al., 2002).

The *ChSCR::GFP* was obtained as follows. The 3 kb region upstream of the *ChSCR* ATG was amplified from *Cardamine* DNA and cloned in pDONR_P4_P1R Gateway vector by BP recombination (Invitrogen). pDONRP4_P1-ChSCRp and pDONR221-ERGFP were recombined with pDONR P2R_P3-NOS into a pB7m34GW destination vector via LR reaction (Invitrogen; Karimi et al., 2002).

35S::MIM165/6 plasmid was obtained from the Nottingham *Arabidopsis* Stock Center (NASC, N783233). *35S::primiR165A* was provided by M. Tsiantis (Max Planck Institute for Plant Breeding Research, Cologne, Germany). Plasmids were introduced into a GV3101 *Agrobacterium tumefaciens* strain and plants were transformed by floral dip (Clough and Bent, 1998). Primers used for plasmid construction are listed in Table S2. Number of transformants obtained are listed in Table S3.

The *ChUB10::GFP* was obtained as follows. The 500 bp region upstream of the *ChUB10* ATG amplified from *Cardamine* DNA and cloned in pDONR_P4_P1R Gateway vector by BP recombination (Invitrogen). pDONRP4_P1-ChUB10p and pDONR221-GFP were recombined with pDONR P2R_P3-NOS into a pB7m34GW destination vector via LR reaction (Invitrogen; Karimi et al., 2002).

The *ChUB10::XPHB* was obtained as follows. The *XPHB* sequence was amplified from *XPHB-PGII* plasmid and cloned in pDONR221 Gateway vector by BP recombination (Invitrogen). Subsequently, pDONRP4_P1R-ChUB10p and pDONR221-XPHB were recombined with pDONR P2R_P3-NOS into a pB7m34GW destination vector via LR reaction (Invitrogen; Karimi et al., 2002).

Microscopy

Confocal images of the median longitudinal sections of the root meristem were taken using a Zeiss LSM 780 microscope. A 10 µg ml^{-1} propidium iodide (Sigma) solution was used to mount the samples and visualize the cell wall.

Differential interference contrast (DIC) with Nomarski technology microscopy (Zeiss Axio Imager A2) was used to image root meristems. Plants were mounted in a chloral hydrate solution (8:3:1 mixture of chloral hydrate:water:glycerol). CEM number is considered as the number of cells from the CEI to the second periclinal division exclusive. Fluorescent signal was measured using Fiji-Image J as described by Moubayidin et al. (2010).

Histology

Casparian strip autofluorescence was analysed as described by Long et al. (2015a).

mPS-PI staining

Ovules were isolated from developing siliques and opened to extract embryos. These were fixed in fixative solution (50% methanol and 10% acetic acid) into a multiwell plate at 4°C overnight. The modified pseudo-Schiff-propidium iodide (mPS-PI) method was performed as described by Truernit et al. (2008).

Real-time PCR

Total RNA was extracted from 5 days post-germination roots using the NucleoSpin RNA Plus (Machery-Nagel), and the first strand cDNA was

synthesized using the Superscript III First Strand Synthesis System (Invitrogen). Quantitative RT-PCR analysis was conducted using the following gene-specific primers: CYCD6;1_RT_F 5′ and CYCD6;1_RT_R 5′ (Sozzani et al., 2010) and qRTPHBfw and qRTPHBrev for *PHB* (Carlsbecker et al., 2010). Relative expression was normalized to ORNITHINE TRANSCARBAMILASE (OTC) control (Dello Ioio et al., 2012).

PCR amplification was carried out in the presence of the double-strand DNA-specific dye SsoAdvanced Universal SYBR Green Supermix (Bio-Rad). Amplification was monitored in real time with the 7500 Fast Real Time PCR System (Applied Biosystems). Experiments were performed in triplicate from two independent root tissue RNA extractions. Data are expressed as $2^{-\Delta\Delta Ct}$ value. Student's *t*-test was used to determine statistical significance of these data (http://graphpad.com/quickcalcs/ttest2.cfm)

Sequences analysis

CDS and protein identity percentage was analysed using ClustalW (www.ebi.ac.uk/Tools/msa/clustalw2/).

Acknowledgements

We acknowledge R. Di Mambro, C. Galinha, M. Cartolano, R. Sozzani, A. Hasson, M. Del Bianco, E. Salvi and E. Pierdonati for valuable discussions on the manuscript; R. Sozzani and Janne Lempe for kindly providing material; and L. Giustini and M. C. Giorgi for technical assistance.

Competing interests

The authors declare no competing or financial interests.

Author contributions

Conceptualization: M.T., S.S., R.D.I.; Methodology: G.D.R., G.B., R.D.I.; Validation: G.D.R., G.B., E.P., L.P., R.D.I.; Formal analysis: G.D.R., G.B., E.P., L.P., R.D.I.; Investigation: G.D.R., G.B., E.P., L.P., R.D.I.; Resources: M.T., S.S., P.C., R.D.I.; Writing - original draft: P.C., R.D.I.; Writing - review & editing: E.P., M.T., P.C., R.D.I.; Visualization: G.D.R., G.B., R.D.I.; Supervision: R.D.I.; Project administration: R.D.I.; Funding acquisition: S.S., P.C., R.D.I.

Funding

This work was supported by a FIRB (Futuro in Ricerca 2013) project grant from the Ministero dell'Istruzione, dell'Università e della Ricerca (FIRB2013-RBFR13DCDS to G.D.R., G.B. and R.D.I.) and a European Research Council grant (260368 to E.P., L.P. and S.S.).

Data availability

Cardamine sequences are available on https://gbrowse.mpipz.mpg.de/cgi-bin/gbrowse/chi1_public/.

Supplementary information

Supplementary information available online at http://dev.biologists.org/lookup/doi/10.1242/dev.153858.supplemental

References

Baulcombe, D. (2004). RNA silencing in plants. *Science* **431**, 356-363.

Benfey, P. N., Linstead, P. J., Roberts, K., Schiefelbein, J. W., Hauser, M. T. and Aeschbacher, R. A. (1993). Root development in Arabidopsis: four mutants with dramatically altered root morphogenesis. *Development* **119**, 57-70.

Carlsbecker, A., Lee, J.-Y., Roberts, C. J., Dettmer, J., Lehesranta, S., Zhou, J., Lindgren, O., Moreno-Risueno, M. A., Vatén, A., Thitamadee, S. et al. (2010). Cell signalling by microRNA165/6 directs gene dose-dependent root cell fate. *Nature* **465**, 316-321.

Clark, N. M., Hinde, E., Winter, C. M., Fisher, A. P., Crosti, G., Blilou, I., Gratton, E., Benfey, P. N. and Sozzani, R. (2016). Tracking transcription factor mobility and interaction in Arabidopsis roots with fluorescence correlation spectroscopy. *Elife* **5**, e14770.

Clough, S. J. and Bent, A. F. (1998). Floral dip: a simplified method for Agrobacterium-mediated transformation of Arabidopsis thaliana. *Plant J.* **16**, 735-743.

Cruz-Ramírez, A., Díaz-Triviño, S., Blilou, I., Grieneisen, V. A., Sozzani, R., Zamioudis, C., Miskolczi, P., Nieuwland, J., Benjamins, R., Dhonukshe, P. et al. (2012). A bistable circuit involving SCARECROW-RETINOBLASTOMA integrates cues to inform asymmetric stem cell division. *Cell* **150**, 1002-1015.

Cui, H., Levesque, M. P., Vernoux, T., Jung, J. W., Paquette, A. J., Gallagher, K. L., Wang, J. Y., Blilou, I., Scheres, B. and Benfey, P. N. (2007). An evolutionarily conserved mechanism delimiting SHR movement defines a single layer of endodermis in plants. *Science* **316**, 421-425.

Dello Ioio, R., Galinha, C., Fletcher, A. G., Grigg, S. P., Molnar, A., Willemsen, V., Scheres, B., Sabatini, S., Baulcombe, D., Maini, P. K. et al. (2012). A PHABULOSA/cytokinin feedback loop controls root growth in Arabidopsis. *Curr. Biol.* **22**, 1699-1704.

Di Laurenzio, L., Wysocka-Diller, J., Malamy, J. E., Pysh, L., Helariutta, Y., Freshour, G., Hahn, M. G., Feldmann, K. A. and Benfey, P. N. (1996). The SCARECROW gene regulates an asymmetric cell division that is essential for generating the radial organization of the Arabidopsis root. *Cell* **86**, 423-433.

Dolan, L., Janmaat, K., Willemsen, V., Linstead, P., Poethig, S., Roberts, K. and Scheres, B. (1993). Cellular organisation of the Arabidopsis thaliana root. *Development* **119**, 71-84.

Fahn, A. (1990). The root. In *Plant Anatomy*, 4th edn, pp. 271-287. Oxford, UK: Pergamon Press.

Gan, X., Hay, A., Kwantes, M., Haberer, G., Hallab, A., Dello Ioio, R., Hofhuis, H., Pieper, B., Cartolano, M., Neumann, U. et al. (2016). Cardamine hirsuta genome offers insight into the evolution of morphological diversity. *Nat. Plants* **2**, 16167.

Grigg, S. P., Galinha, C., Kornet, N., Canales, C., Scheres, B. and Tsiantis, M. (2009). Repression of apical homeobox genes is required for embryonic root development in Arabidopsis. *Curr. Biol.* **19**, 1485-1490.

Hay, A. and Tsiantis, M. (2006). The genetic basis for differences in leaf form between Arabidopsis thaliana and its wild relative Cardamine hirsuta. *Nat. Genet.* **38**, 942-947.

Hay, A. S., Pieper, B., Cooke, E., Mandáková, T., Cartolano, M., Tattersall, A. D., Dello Ioio, R., McGowan, S. J., Barkoulas, M., Galinha, C. et al. (2014). Cardamine hirsuta: a versatile genetic system for comparative studies. *Plant J.* **78**, 1-15.

Heidstra, R., Welch, D. and Scheres, B. (2004). Mosaic analyses using marked activation and deletion clones dissect Arabidopsis SCARECROW action in asymmetric cell division. *Genes Dev.* **18**, 1964-1969.

Heimsch, C. and Seago, J. L.Jr. (2008). Organization of the root apical meristem in angiosperms. *Am. J. Bot.* **95**, 1-21.

Helariutta, Y., Fukaki, H., Wysocka-Diller, J., Nakajima, K., Jung, J., Sena, G., Hauser, M.-T. and Benfey, P. N. (2000). The SHORTROOT gene controls radial patterning of the Arabidopsis root through radial signaling. *Cell* **101**, 555-567.

Henry, S., Dievart, A., Divol, F., Pauluzzi, G., Meynard, D., Swarup, R., Wu, S., Gallagher, K. L. and Périn, C. (2017). SHR overexpression induces the formation of supernumerary cell layers with cortex cell identity in rice. *Dev. Biol.* **425**, 1-7.

Heo, J.-O., Chang, K. S., Kim, I. A., Lee, M.-H., Lee, S. A., Song, S.-K., Lee, M. M. and Lim, J. (2011). Funneling of gibberellin signaling by the GRAS transcription regulator scarecrow-like 3 in the Arabidopsis root. *Proc. Natl. Acad. Sci. USA.* **108**, 2166-2171.

Hofhuis, H., Moulton, D., Lessinnes, T., Routier-Kierzkowska, A.-L., Bomphrey, R. J., Mosca, G., Reinhardt, H., Sarchet, P., Gan, X., Tsiantis, M. et al. (2016). Morphomechanical innovation drives explosive seed dispersal. *Cell* **166**, 222-233.

Karimi, M., Inzé, D. and Depicker, A. (2002). GATEWAY™ vectors for Agrobacterium-mediated plant transformation. *Trends Plant Sci.* **7**, 193-195.

Kirschner, G. K., Stahl, Y., Von Korff, M. and Simon, R. (2017). Unique and conserved features of the barley root meristem. *Front. Plant Sci.* **8**, 1240.

Koizumi, K., Hayashi, T., Wu, S. and Gallagher, K. L. (2012). The SHORT-ROOT protein acts as a mobile, dose-dependent signal in patterning the ground tissue. *Proc. Natl. Acad. Sci. USA* **109**, 13010-13015.

Long, Y., Goedhart, J., Schneijderberg, M., Terpstra, I., Shimotohno, A., Bouchet, B. P., Akhmanova, A., Gadella, T. W., Jr, Heidstra, R., Scheres, B. et al. (2015a). SCARECROW-LIKE23 and SCARECROW jointly specify endodermal cell fate but distinctly control SHORT-ROOT movement. *Plant J.* **84**, 773-784.

Long, Y., Smet, W., Cruz-Ramírez, A., Castelijns, B., de Jonge, W., Mähönen, A. P., Bouchet, B. P., Perez, G. S., Akhmanova, A., Scheres, B. et al. (2015b). Arabidopsis BIRD zinc finger proteins jointly stabilize tissue boundaries by confining the cell fate regulator SHORT-ROOT and contributing to fate specification. *Plant Cell* **27**, 1185-1199.

Long, Y., Stahl, Y., Weidtkamp-Peters, S., Postma, M., Zhou, W., Goedhart, J., Sánchez-Pérez, M. I., Gadella, T. W. J., Simon, R., Scheres, B. et al. (2017). In vivo FRET-FLIM reveals cell-type-specific protein interactions in Arabidopsis roots. *Nature* **548**, 97-102.

Lu, C. and Fedoroff, N. (2000). A mutation in the Arabidopsis HYL1 gene encoding a dsRNA binding protein affects responses to abscisic acid, auxin, and cytokinin. *Plant Cell* **12**, 2351-2366.

Mallory, A. C., Reinhart, B. J., Jones-Rhoades, M. W., Tang, G., Zamore, P. D., Barton, M. K. and Bartel, D. P. (2004). MicroRNA control of *PHABULOSA* in leaf development: importance of pairing to the microRNA 5′ region. *EMBO J.* **23**, 3356-3364.

McConnell, J. R., Emery, J., Eshed, Y., Bao, N., Bowman, J. and Barton, M. K. (2001). Role of PHABULOSA and PHAVOLUTA in determining radial patterning in shoots. *Nature* **411**, 709-713.

Miyashima, S., Hashimoto, T. and Nakajima, K. (2009). ARGONAUTE1 acts in Arabidopsis root radial pattern formation independently of the SHR/SCR pathway. *Plant Cell Physiol.* **50**, 626-634.

Miyashima, S., Koi, S., Hashimoto, T. and Nakajima, K. (2011). Non-cell-autonomous microRNA165 acts in a dose-dependent manner to regulate multiple differentiation status in the *Arabidopsis* root. *Development* **138**, 2303-2313.
Miyashima, S., Honda, M., Hashimoto, K., Tatematsu, K., Hashimoto, T., Sato-Nara, K., Okada, K. and Nakajima, K. (2013). A comprehensive expression analysis of the Arabidopsis MICRORNA165/6 gene family during embryogenesis reveals a conserved role in meristem specification and a non-cell-autonomous function. *Plant Cell Phys.* **54**, 375-384.
Morel, J.-B., Godon, C., Mourrain, P., Béclin, C., Boutet, S., Feuerbach, F., Proux, F. and Vaucheret, H. (2002). Fertile hypomorphic ARGONAUTE (ago1) mutants impaired in post-transcriptional gene silencing and virus resistance. *Plant Cell* **14**, 629-639.
Moreno-Risueno, M. A., Sozzani, R., Yardımcı, G. G., Petricka, J. J., Vernoux, T., Blilou, I., Alonso, J., Winter, C. M., Ohler, U., Scheres, B. et al. (2015). Transcriptional control of tissue formation throughout root development. *Science* **350**, 426-430.
Moubayidin, L., Perilli, S., Dello Ioio, R., Di Mambro, R., Costantino, P. and Sabatini, S. (2010). The rate of cell differentiation controls the Arabidopsis root meristem growth phase. *Curr. Biol.* **12**, 1138-1143.
Paquette, A. J. and Benfey, P. N. (2005). Maturation of the ground tissue of the root is regulated by gibberellin and SCARECROW and requires SHORT-ROOT. *Plant Physiol.* **138**, 636-640.
Park, M. Y., Wu, G., Gonzalez-Sulser, A., Vaucheret, H. and Poethig, R. S. (2005). Nuclear processing and export of microRNAs in Arabidopsis. *Proc. Natl. Acad. Sci. USA* **102**, 3691-3696.
Pauluzzi, G., Divol, F., Puig, J., Guiderdoni, E., Dievart, A. and Périn, C. (2012). Surfing along the root ground tissue gene network. *Dev. Biol.* **365**, 14-22.
Perilli, S. and Sabatini, S. (2010). Analysis of root meristem size development. *Methods Mol. Biol.* **655**, 177-187.
Prigge, M. J., Otsuga, D., Alonso, J. M., Ecker, J. R., Drews, G. N. and Clark, S. E. (2005). Class III homeodomain-leucine zipper gene family members have overlapping, antagonistic, and distinct roles in arabidopsis development. *Plant Cell* **17**, 61-76.
Rast-Somssich, M. I., Broholm, S., Jenkins, H., Canales, C., Vlad, D., Kwantes, M., Bilsborough, G., Dello Ioio, R., Ewing, R. M., Laufs, P. et al. (2015). Alternate wiring of a KNOXI genetic network underlies differences in leaf development of A. thaliana and C. hirsuta. *Genes Dev.* **29**, 2391-2404.
Scheres, B., Wolkenfelt, H., Willemsen, V., Terlouw, M., Lawson, E., Dean, C. and Weisbeek, P. (1994). Embryonic origin of the Arabidopsis primary root and root meristem initials. *Development* **120**, 2475-2487.
Scheres, B., Di Laurenzio, L., Willemsen, V., Hauser, M. T., Janmaat, K., Weisbeek, P. and Benfey, P. N. (1995). Mutations affecting the radial organisation of the Arabidopsis root display specific defects throughout the embryonic axis. *Development* **121**, 53-62.
Skopelitis, D. S., Husbands, A. Y. and Timmermans, M. C. P. (2012). Plant small RNAs as morphogens. *Curr. Opin. Cell Biol.* **24**, 217-224.
Sozzani, R., Cui, H., Moreno-Risueno, M. A., Busch, W., Van Norman, J. M., Vernoux, T., Brady, S. M., Dewitte, W., Murray, J. A. H. and Benfey, P. N. (2010). Spatiotemporal regulation of cell-cycle genes by SHORTROOT links patterning and growth. *Nature* **466**, 128-132.
Telfer, A. and Poethig, R. S. (1998). HASTY: a gene that regulates the timing of shoot maturation in Arabidopsis thaliana. *Development* **125**, 1889-1898.
Todesco, M., Rubio-Somoza, I., Paz-Ares, J. and Weigel, D. (2010). A collection of target mimics for comprehensive analysis of microRNA function in Arabidopsis thaliana. *PLoS Genet.* **6**, e1001031.
Truernit, E., Bauby, H., Dubreucq, B., Grandjean, O., Runions, J., Barthélémy, J. and Palauqui, J.-C. (2008). High-resolution whole-mount imaging of three-dimensional tissue organization and gene expression enables the study of Phloem development and structure in Arabidopsis. *Plant Cell* **20**, 1494-1503.
Vlad, D., Kierzkowski, D., Rast, M. I., Vuolo, F., Dello Ioio, R., Galinha, C., Gan, X., Hajheidari, M., Hay, A., Smith, R. S. et al. (2014). Leaf shape evolution through duplication, regulatory diversification, and loss of a homeobox gene. *Science* **343**, 780-783.
Vuolo, F., Mentink, R. A., Hajheidari, M., Bailey, C. D., Filatov, D. A. and Tsiantis, M. (2016). Coupled enhancer and coding sequence evolution of a homeobox gene shaped leaf diversity. *Genes Dev.* **30**, 2370-2375.
Welch, D., Hassan, H., Blilou, I., Immink, R., Heidstra, R. and Scheres, B. (2007). Arabidopsis JACKDAW and MAGPIE zinc finger proteins delimit asymmetric cell division and stabilize tissue boundaries by restricting SHORT-ROOT action. *Genes Dev.* **21**, 2196-2204.
Wu, S., Lee, C.-M., Hayashi, T., Price, S., Divol, F., Henry, S., Pauluzzi, G., Perin, C. and Gallagher, K. L. (2014). A plausible mechanism, based upon Short-Root movement, for regulating the number of cortex cell layers in roots. *Proc. Natl. Acad. Sci. USA* **111**, 16184-16189.
Wysocka-Diller, J. W., Helariutta, Y., Fukaki, H., Malamy, J. E. and Benfey, P. N. (2000). Molecular analysis of SCARECROW function reveals a radial patterning mechanism common to root and shoot. *Development* **127**, 595-603.
Zhang, Z.-L., Ogawa, M., Fleet, C. M., Zentella, R., Hu, J., Heo, J.-O., Lim, J., Kamiya, Y., Yamaguchi, S. and Sun, T.-P. (2011). Scarecrow-like 3 promotes gibberellin signaling by antagonizing master growth repressor DELLA in Arabidopsis. *Proc. Natl. Acad. Sci. USA* **108**, 2160-2165.